

Preparation of Cellulose Nanocrystals *via* Successive Periodate and Bisulfite Oxidation and Mechanical and Hydrophilic Properties of the Films

Baoyu Wang,^a Rong Li,^a Jinhao Zeng,^a Min He,^a and Junrong Li^{b,*}

Microcrystalline cellulose was oxidized *via* periodate followed by sulfonation. The sulfonated cellulose nanocrystals were obtained through centrifugation, dialysis, and sonication. The sulfonated cellulose nanocrystals were rod-like and had an average length of 140 nm to 153 nm and an average width of 8 to 10 nm. The Fourier transform infrared profiles and polyelectrate titration demonstrated successful introduction of the sulfonated groups into the cellulose nanocrystals. The sulfonated cellulose nanocrystals had a higher crystallinity index than dialdehyde cellulose. The thin films fabricated *via* the casting of the sulfonated cellulose nanocrystals suspensions were highly hydrophilic.

Keywords: Sulfonated cellulose; Nanocrystal; Hydrophilicity

Contact information: a: School of Chemical Engineering and Technology, Guangdong Industry Polytechnic, Guangzhou 510300 China; b: State Key Laboratory of Pulp and Paper Engineering, South China University of Technology, Guangzhou 510640 China; *Corresponding author: lljrr@scut.edu.cn

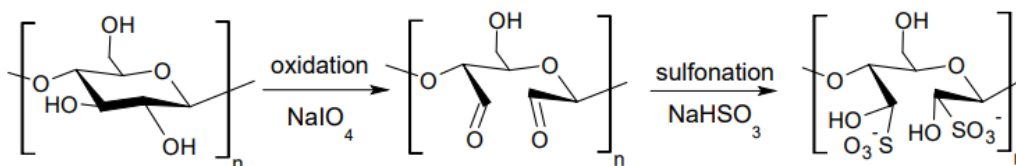
INTRODUCTION

Cellulose is the primary component of the cell walls of plants and algae and is the most abundant natural polymer found in nature (Klemm *et al.* 2005). This bio-based material has low toxicity, it is biocompatible and renewable, and there is a growing interest to replace petrochemical products with cellulose to alleviate environment pollution (Goetz *et al.* 2009). Nanocellulose refers to cellulose particles having at least one dimension in nanoscale (1 nm to 100 nm), which are usually classified as cellulose nanocrystals (CNC) or cellulose nanofibril (CNF). Cellulose nanocrystals are rod-like with a length of 200 nm to 500 nm and a diameter of 3 nm to 35 nm and can be derived from acidic hydrolysis. However, the acidic hydrolysis process causes problems, *e.g.*, equipment erosion and environmental pollution (Rånby *et al.* 1949). Cellulose nanofibril particles have a diameter of 5 nm to 50 nm and a length of a few micrometers and can be obtained *via* chemical or enzymatic pretreatment, followed by mechanical treatment. However, mechanical treatment consumes a lot of energy (Nechporchuk *et al.* 2016).

It is well known that cellulose can be oxidized with periodate to obtain dialdehyde cellulose (DAC), which occurs when the C₂-C₃ bonds are broken and the hydroxyl groups at C₂ and C₃ are converted into aldehyde groups (Kim *et al.* 2000). The opening of the β-D glucose units disrupts the ordered structure of cellulose, and the flexibility of the cellulose chain dramatically increases (Casu *et al.* 1985). Meanwhile, DAC is a highly active intermediate, which can be further derivatized into dialcohol, dicarboxylate, imine, and sulfonate cellulose (Guigo *et al.* 2014). In recent years, CNC has been separated *via* derivative reactions of DAC. Errokh *et al.* (2018) obtained CNC with a width of 5 nm to 10 nm *via* the NaBH₄ reduction of DAC. Yang *et al.* (2013) separated CNC with a length

of 120 to 200 nm and a diameter of approximately 13 nm *via* the chlorite oxidation of DAC. Visanko *et al.* (2014) used a combined procedure of the reductive amination of DAC and its mechanical homogenization to synthesize CNC with both hydrophobic and hydrophilic properties.

The sulfonation of DAC (shown as scheme 1) introduces sulfonated groups into the DAC molecular chains, and the electrostatic force between sulfonated groups acts on the DAC particles, CNC should be obtained *via* the sulfonation of DAC. However, there are only reports concerning CNF produced *via* the sulfonation of DAC and the solubility of sulfonated cellulose. Sun *et al.* (2017) separated CNF *via* the sulfonation of DAC followed by homogenization, which can be used as an oil/water separator. Pan and Ragauskas (2014) produced CNFs with a width of 15 nm to 45 nm and length of 1 μm following the same procedure. Thiangtham *et al.* (2019) obtained transparent sulfonated suspensions *via* the sulfonation of DAC and found the suspensions contained cellulose particles, but unfortunately there was no further exploration of these particles.



Scheme 1. Sulfonation of DAC

Sulfonated cellulose is a potential immunosorbent material (Rocha *et al.* 2018) and green flocculation agent for mineral particles (Liimatainen *et al.* 2013). Sulfonated cellulose film has a potential application as a separator membrane in lithium-ion batteries (Thiangtham *et al.* 2019). The purpose of this study was to extract sulfonated nanocrystals (SCNCs) *via* the sulfonation of DAC. Microcrystalline cellulose (MCC) was first oxidized to DAC with a moderate dialdehyde content, followed by sulfonation with sodium bisulfite. Fourier-transform infrared spectroscopy (FTIR), X-ray diffraction (XRD), and atomic force microscopy (AFM) were used to characterize SCNCs. The films were fabricated *via* the casting of SCNCs suspensions, and the mechanical strength and hydrophilicity of the films were investigated.

EXPERIMENTAL

Raw Materials

The MCC (particle size less than 25 μm), sodium periodate, sodium hydroxide, and ammonium hydrochloride were purchased from Aladdin (Shanghai, China). The sodium chlorite, glacial acetic acid, sodium bisulfite, ethylene glycol, and poly (diallyl-dimethylammonium chloride) (PDADMAC) were purchased from Macklin (Shanghai, China). All the chemicals were of analytical grade or above and used as received. Deionized water was used throughout the experiments.

Extraction of Sulfonate Nanocrystals

Preparation of DAC

The MCC was oxidized to DAC following the process outlined by Sirviö *et al.* (2011) with some changes. In summary, 4 g of MCC, 5.28 g of NaIO_4 (molar ratio of NaIO_4

to AGU = 1 to 1), 3.364 g of sodium chloride (molar ratio of NaCl to AGU = 7 to 3), and 200 mL of deionized water were added into a conical flask covered with aluminum foil and the mixture was magnetically stirred in a water bath at 50 °C for 3 h, followed by the addition of ethylene glycol to terminate the reaction. Subsequently, the suspension was vacuum filtered and washed several times with deionized water until the conductivity was less than 50 $\mu\text{S}/\text{cm}$, then rinsed with ethanol. Finally, the oxidized products were vacuum dried and stored for further use.

Sulfonation of DAC

The sulfonation of DAC was performed according to the following procedure: 2 g of DAC, 2 g of sodium bisulfite (19.2 mM), and 200 mL of deionized water were mixed together and magnetically stirred at room temperature for 6 h, 12 h, and 24 h to obtain the sulfonated cellulose samples correspondingly named SCNC₁, SCNC₂, and SCNC₃.

Separation of nanocrystals

The sulfonated cellulose was first centrifuged twice at 10000 rpm for 10 min; the sediment was collected and dialyzed (molecular weight cut-off (MWCO) = 8 kDa to 14 kDa) against deionized water until the conductivity was less than 50 $\mu\text{S}/\text{cm}$. Subsequently, the dialyzed suspension was sonicated for 10 min at a power of 650 W and an amplitude of 80%, and then centrifuged at 10000 rpm for 10 min to remove any fiber bundles. Finally, the supernatant was collected for further use.

Determination of Aldehyde Group Content

The aldehyde group content of DAC was determined following the literature procedure (Zhao and Heindel 1991).

Charge Density Measurements

The charge density of the SCNCs was determined using a particle charge analyzer (PCD-05, BTG Instruments, Värmland, Sweden). The suspension of the sulfonated cellulose was diluted 10-fold, and 10 mL of the diluted suspension was pipetted into the measurement cell and then titrated with 0.001 N of PDADMAC.

Characterization of the Sulfonated Cellulose Nanocrystals (SCNCs)

The FTIR measurements were carried out with a FTIR spectrometer (Thermo Scientific Nicolet 6700, Waltham, MA); the spectra of the samples were obtained *via* KBr pellets in transmission mode. The XRD measurements were performed with an X-ray fluorescence spectrometer (AXIOS-PW4400, Malvern Panalytical, Malvern, United Kingdom) using Cu K α ($\lambda = 1.5406$ nm) radiation. The crystalline index (CI) was evaluated based on the Segal method (Segal *et al.* 1959).

The morphology of the SCNCs were investigated with an atomic force microscope (AFM) (Nanoscope IIIa, Veeco, Plainview, NY) with silicon cantilever probes in tapping mode; the images were analyzed with Nanoscope Analysis software (version 1.7, Bruker, Billerica, MA). The dimensions of the SCNCs were determined with a nanoparticle analyzer (SZ-100, Horiba, Kyoto, Japan). The scattering angle was 90° and six tests were conducted for each sample. The Z-average diameter and polydispersity index were averaged for each sample.

Mechanical Strength of the Sulfonated Cellulose Nanocrystals (SCNCs) Films

The SCNCs suspension with a consistency of 0.2% was cast in polystyrene Petri dishes at 50 °C. After conditioned for 24 h, the films were cut into strips with a length of 35 mm and a width of 15 mm. The thickness of strips was measured with L&W micrometer (Lorentzen & Wettre, Stockholm, Sweden). The tests to determine the mechanical properties were performed with a tensile and compression tester (Instron 5565, Instron, Norwood, MA) equipped with a 500 N load cell, and a crosshead span of 20 mm and a strain rate of 4 mm/min were set for the tests. The tensile strength, Young's modulus, and strain at break were recorded.

Contact Angle Analysis of the Sulfonated Cellulose Nanocrystals (SCNCs) Films

The hydrophilic property of the films was examined *via* a contact angle meter (SL200KB, Kino Industry Co., Ltd. Boston, MA). Deionized water was used as the probe liquid. A droplet of water (2 µL) was dropped onto the film surface, the images of the droplet were captured with a digital camera, and the contact angle was automatically calculated with the drop shape analysis system CAST 3.0 (Kino Industry Co. Ltd. Boston, MA).

RESULTS AND DISCUSSION

Oxidation and Sulfonation of the Microcrystalline Cellulose (MCC)

In this study, cellulose nanocrystals were separated from MCC *via* successive periodate oxidation and bisulfite sulfonation. The MCC was first oxidized *via* sodium periodate to form DAC with an aldehyde groups content of 4.32 mmol/g. Metallic salts and an elevated temperature can accelerate the oxidation reaction; thus, a higher aldehyde content can be achieved in comparison to an oxidation process at room temperature without the addition of salts (Sirviö *et al.* 2011). However, including metallic salts and having a higher temperature promotes DAC chain breakdown and increases the solubility of DAC (Kim *et al.* 2004), which led to an oxidation yield of only 67.3%.

A stable and homogenous suspension was obtained after the DAC samples were sulfonated for 6, 12, and 24 h, respectively, and these nanocrystals suspensions were visually evaluated with the Tyndall effect, which refers to a bright light beam is visible as a beam of light passes through a colloid suspension (Voskoboinikov *et al.* 2011). There was weak Tyndall effect presented in the SCNC₁ suspension, as shown in Fig.1 (B). In order to obtain the nanocrystals, the suspension was centrifuged twice, and the gel at the bottom of the tube was collected. After dilution, dialysis, centrifugation, and sonication, the collected gel became a stable, clear, and transparent suspension, and displayed the Tyndall effect, as shown in Fig. 1(D). The SCNCs yield from the MCC sulfonated for 6, 12, and 24 h were 54.4%, 51.6%, and 45.8% respectively, *i.e.*, the longer the sulfonation, the greater the mass loss. The mass loss may be caused by the dissolution of the amorphous part during the sulfonation step, and the yield was lower than reported by Rajalaxmi *et al.* (2010) (the yield was 87% to 94%). This was probably due to the lower aldehyde content of DAC (0.28 mmol/g), compared to the aldehyde content in this study (4.32 mmol/g).

In addition, the suspension was difficult to filter. There was no filtrate at all when the suspension was filtered with a hydrophilic MCE membrane (a pore size of $0.65\ \mu\text{m}$) under a vacuum pressure of $0.08\ \text{MPa}$, which indicated that the sulfonated cellulose possessed a strong capability of absorbing water. Therefore, the suspension was purified *via* dialysis.

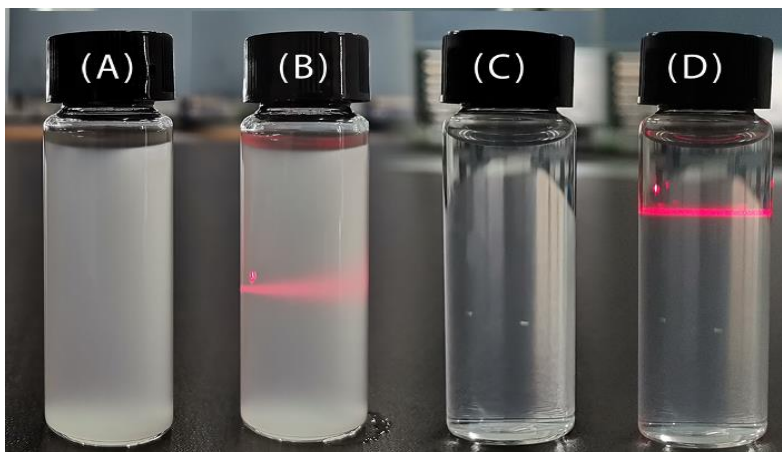


Fig. 1. Photographs of the SCNC₁ suspensions without laser illumination (A) and with laser illumination (B); the SCNC₁ suspension after sonication without laser illumination (C) and with laser illumination (D)

Fourier Transform Infrared (FTIR) Analysis

The changes in the chemical structure were investigated *via* FTIR. The results are shown in Fig. 2. The weak peak at $1726\ \text{cm}^{-1}$ was identified as the characteristic band of an aldehyde group, and the band at $891\ \text{cm}^{-1}$ was attributed to hemiacetal and hydrate aldehyde (Speddin 1960; Sabzalian *et al.* 2014), which demonstrated the successful conversion of MCC into DAC. In the case of the SCNCs samples, the weak peaks at the $1160\ \text{cm}^{-1}$ and $1115\ \text{cm}^{-1}$ bands were regarded as symmetric and asymmetric of stretching of the S=O bonds (Suganuma *et al.* 2008). However, the peaks at the $1726\ \text{cm}^{-1}$ and $891\ \text{cm}^{-1}$ bands appeared on all the sulfonated celluloses, which indicated that only a part of the aldehyde groups were converted into SO_3^- groups.

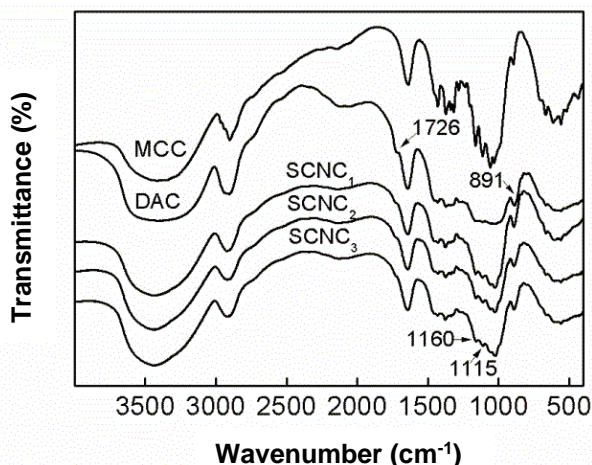


Fig. 2. FTIR spectra of the samples

Polyelectrate Titration

The charge densities of the SCNCs were determined *via* polyelectrate titration. The charge densities of the SCNC₁, SCNC₂, and SCNC₃ samples were found to be -0.44, -0.57, and -0.75 meq/g, respectively, which revealed that more aldehyde groups were converted into sulfonated groups with a longer sulfonation reaction. The negative sulfonated groups established an electrostatic repulsion effect between the SCNCs and played an important role in the stability of the sulfonated cellulose suspensions, which appeared clear, transparent, and homogenous even after 3 months of storage. The results indicated that a stable sulfonated cellulose suspensions could be obtained *via* the sulfonation of DAC at an equal dosage of NaHSO₃ (mass ratio of DAC to NaHSO₃ = 1 to 1) at room temperature for 6 h.

Morphology of the Sulfonated Cellulose Nanocrystals (SCNCs)

Dialdehyde cellulose is insoluble in water due to the hemiacetals and acetyls in its cellulosic structure (Kim *et al.* 2004). However, the dissolution of some of the DAC amorphous regions enabled the liberation of CNC during the amination process of DAC (Sirviö *et al.* 2016). The mechanisms for the liberation of the SCNCs *via* the sulfonation of DAC may be the same as the DAC amination procedure. The morphologies of the SCNC₂ and SCNC₃ samples are presented in Fig. 3.

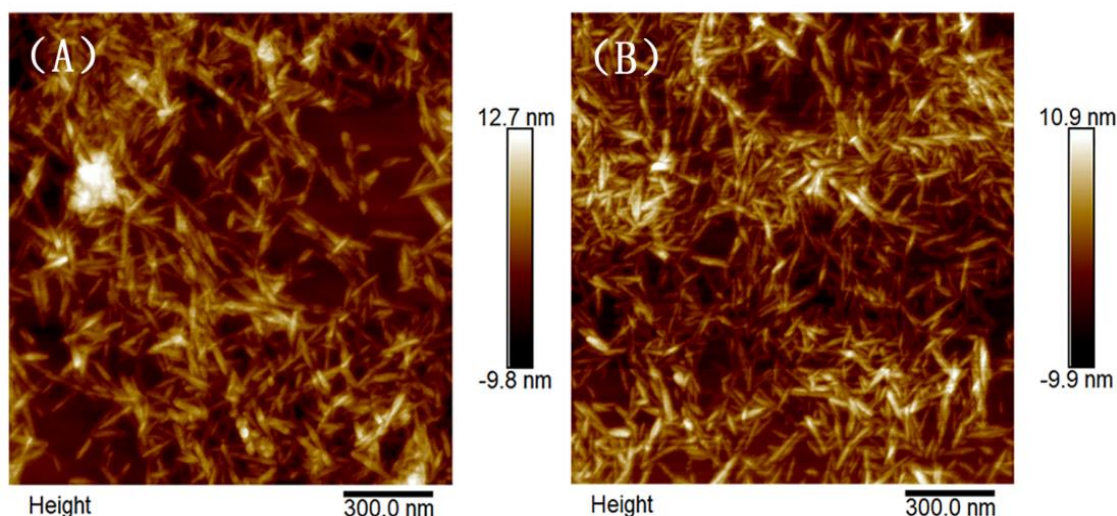


Fig. 3. AFM height images of SCNC₂ (A); and SCNC₃ (B)

The SCNCs were rod-like and tended to aggregate. The average length of the SCNC₂ and SCNC₃ nanoparticles was $152.5 \text{ nm} \pm 55.9 \text{ nm}$ and $142 \text{ nm} \pm 29.4 \text{ nm}$, respectively, and the average width was $9.47 \text{ nm} \pm 1.70 \text{ nm}$ and $8.68 \text{ nm} \pm 1.43 \text{ nm}$, respectively. Both the morphology and the dimensions of the SCNCs were similar to the morphology and the dimensions of the CNC samples derived *via* sulfuric acid hydrolysis (Dong *et al.* 1998) and the morphology and the dimensions of the CNC derived *via* a successive periodate oxidation and heating treatment (Yang *et al.* 2015).

Particle Size Analysis

The size of the SCNCs was also determined *via* dynamic light scattering (DLS) and the results are presented in Fig. 4. The Z-average size of the SCNC₁, SCNC₂, and SCNC₃

samples were $266.1 \text{ nm} \pm 14 \text{ nm}$, $168.2 \text{ nm} \pm 4.5 \text{ nm}$, and $111.1 \text{ nm} \pm 4.1 \text{ nm}$, respectively, which were close to size of the nanocrystals extracted *via* successive periodate and chlorite oxidation (Yang *et al.* 2013). The results indicated that the longer the sulfonation reaction, the smaller the SCNCs particles. The polydispersity indexes of the SCNC₁, SCNC₂, and SCNC₃ samples were 0.434 ± 0.05 , 0.434 ± 0.02 , and 0.412 ± 0.08 , which revealed that the longer the sulfonation reaction, the more uniform the dimensions of the SCNCs.

In addition, only one peak was recorded in the DLS profiles for all SCNCs samples, whereas the acid hydrolysis subjected CNCs exhibited two peaks due to the orientation of rod-shaped CNCs (Shanmugarajah *et al.* 2015). One peak distribution possibly originated from the aggregation of the SCNCs. The DLS profile of the CNC separated *via* successive periodate and NaBH₄ reduction also showed a one peak distribution (Errokh *et al.* 2018). Both the DLS and AFM results demonstrated that the dimensions of the SCNCs tended to become smaller as the sulfonation reaction time increased.

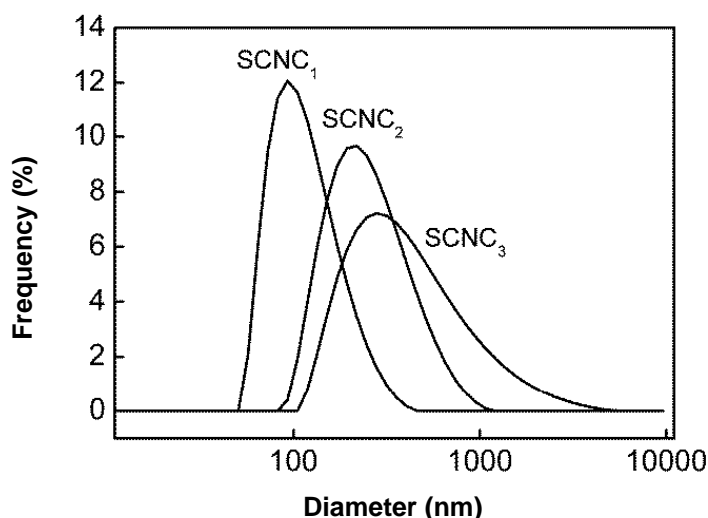


Fig. 4. Size and distribution of the SCNCs particles determined *via* DLS

Determination of the Crystalline Index *via* X-Ray Diffraction (XRD)

The XRD profiles of the sulfonated cellulose (SC) samples are presented in Fig. 5. All the diffractograms exhibited typical peaks at 14.5° , 16.5° , and 22.6° , which corresponded to Bragg angles of $1\bar{1}0$, 110, and 200 crystalline planes respectively. This indicated that the SCNCs had the same polymorphs as cellulose I (Sirviö *et al.* 2011; Yang *et al.* 2013; Sun *et al.* 2015). When the MCC was oxidized with periodate, the glucopyranose rings opened and the ordered structures were destroyed, which led to a decrease in the CI, from 82.5% for MCC to 41.6% for DAC, which was in agreement with the report by Kim *et al.* (2000).

In the sulfonation step, the hemiacetal bonds were disrupted, and the amorphous parts of the cellulose were dissolved. Therefore, the CI of the SCNC₁, SCNC₂, and SCNC₃ samples increased to 56.4%, 62.6%, and 64.1%, respectively, which was confirmed by the decrease in the yield of the sulfonation reaction. The longer the sulfonation reaction, the more the amorphous parts were dissolved and the higher the CI of the SCNCs. Erokh *et al.* (2018) also reported an increase in CI during the NaBH₄ reduction of DAC.

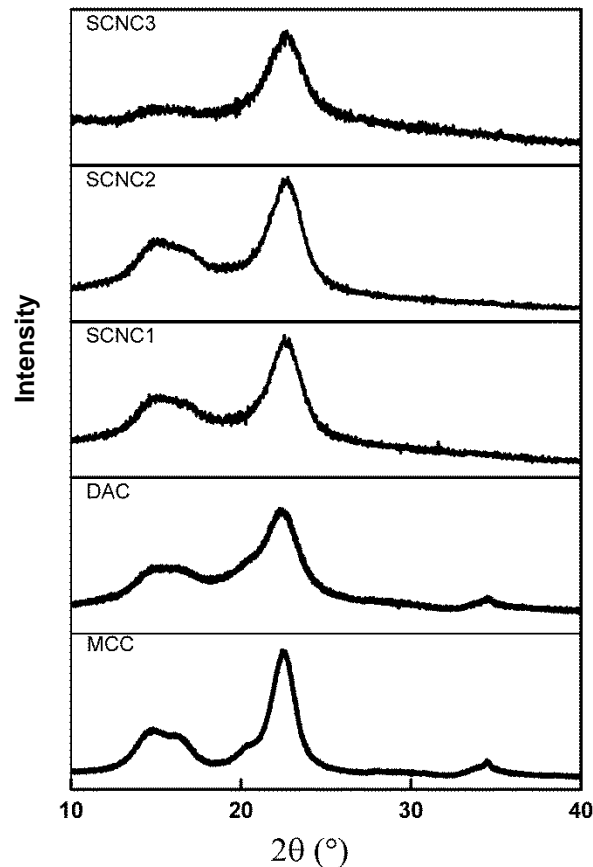


Fig. 5. The diffractograms of the SCNCs

Mechanical Strength of the Films

Highly transparent films were obtained *via* the casting of the SCNCs suspensions, and the films are shown in Fig. 6. The thickness of these films ranged from 30 μm to 45 μm . The films cast from SCNC₂ and SCNC₃ were so brittle that cracks appeared at the edges of the films when they were cut into strips, which may be ascribed to a higher crystallinity index (56.4% for SCNC₁, 62.6% for SCNC₂ and 64.1% for SCNC₃) and a relatively small size of the nanocrystals (Z-average size of SCNC₁, SCNC₂, and SCNC₃ were 266.1, 168.2, and 111.1 nm), so only the mechanical properties of the SCNC₁ films were obtained. The Young's modulus, tensile strength, and strain at break of the SCNC₁ film were 4.12 GPa \pm 0.43 GPa, 49 MPa \pm 5 MPa, and 1.69% \pm 0.14%, respectively, as shown in Fig. 7. Visanko *et al.* (2015) extracted CNC (ADCNC) with an aspect ratio of 50 *via* the amination of DAC, and Bras *et al.* (2011) extracted CNC (AHCNC) with an aspect ratio of 11.3 *via* acid hydrolysis. The Young's modulus of the ADCNC and AHCNC films were 5.7 and 2.14 GPa, respectively. The SCNCs in this paper were rigid and rod-like, which was the same as the ADCNC and AHCNC. For the rigid and rod-like CNC, the aspect ratio plays an important role in terms of Young's modulus; the higher the aspect ratio, the higher the Young's modulus (Bras *et al.* 2011). The Young's modulus of the SCNCs film was lower than the Young's modulus of the ADCNC film, which was due to the lower aspect ratio of the SCNCs (16.7). The aspect ratio of the SCNCs and AHCNC

were similar; the higher Young's modulus of the SCNCs film was ascribed to hemiacetyl cross-linking and a higher aspect ratio. Liimatainen and Visanko (2013) prepared CNF, with a width of 10 to 60 nm and a length of several micrometers, *via* the sulfonation of DAC followed by homogenization. This CNF film had a Young's modulus of 13.5 GPa, which was much higher than the Young's modulus of the SCNC₁ film. The CNF was flexible and had a large aspect ratio and was able to entangle each other during the process of film formation, so the CNF films had a higher Young's modulus than the SCNC₁ film.

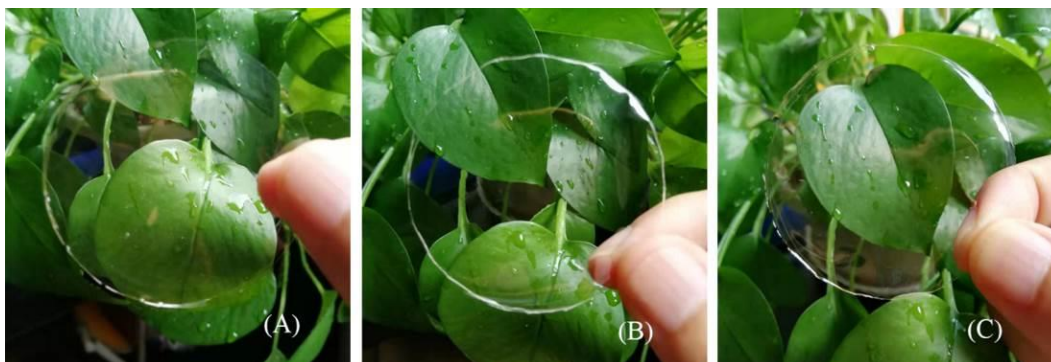


Fig. 6. Appearance of the transparent SCNC₁ film (A); SCNC₂ film (B); and SCNC₃ film (C)

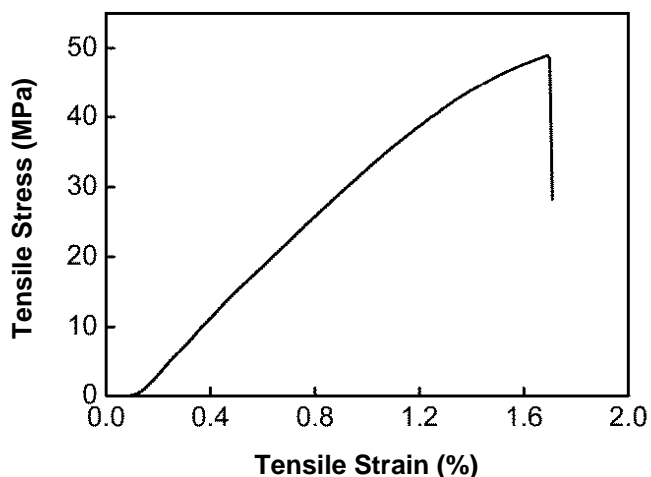


Fig 7. Stress vs. strain of the SCNC₁ film

Hydrophilicity of the Films

The hydrophilic property of the SCNCs films was evaluated *via* dynamic contact angle tests, and the results are presented in Fig. 8. The initial contact angles of the SCNC₁, SCNC₂, and SCNC₃ samples were $33.7^\circ \pm 5.1^\circ$, $30.63^\circ \pm 4.3^\circ$, and $27.4^\circ \pm 4.8^\circ$, respectively. Compared with DCC, which had a contact angle of 45° (Visanko *et al.* 2014), and TEMPO nanofibrils, which had a contact angle of 52° (Rodionova *et al.* 2012), the SCNCs films had the lowest contact angle. The value of the contact angle of the films decreased as the sulfonated group content increased. The results indicated that the SCNCs were highly hydrophilic, and the hydrophilicity was ascribed to a large number of hydroxyl and sulfonated groups on the surface of the SCNCs.

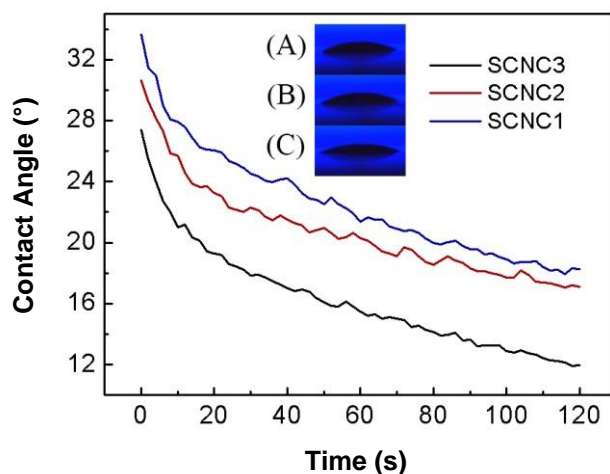


Fig. 8. Dynamic contact angle plot of SCNCs films and photographs of the initial contact angle of SCNC₁ (A), SCNC₂ (B) and SCNC₃ (C)

CONCLUSIONS

1. Microcrystalline cellulose was oxidized with sodium periodate followed by sulfonation with sodium bisulfite, and a stable, transparent, and homogenous sulfonated cellulose suspension was obtained.
2. The rod-like sulfonated cellulose nanocrystals (SCNCs), which had an average length of 140 nm to 153 nm and an average width of 8 to 10 nm, were extracted *via* dialysis, centrifugation, and sonication of the sulfonated cellulose suspension.
3. Compared with dialdehyde cellulose (DAC), the SCNCs had a higher crystalline index, which ranged from 56% to 64%.
4. The SCNCs films are transparent and had a Young's modulus of 4.12 GPa and a tensile strength of 49 MPa. In addition, the SCNCs film was highly hydrophilic and the contact angle of the SCNCs films reached a minimum of 27.4°

ACKNOWLEDGMENTS

The authors sincerely acknowledge and appreciate the funding support by the Guangdong Industry Polytechnic Research Team Program (Grant No. KYTD2018-005) and the Guangdong Industry Polytechnic Natural Science Foundation Program (Grant No. KYTD2019-008)

REFERENCES CITED

- Bras, J., Viet, D., Bruzzese, C., and Dufresne, A. (2011). "Correlation between stiffness of sheets prepared from cellulose whiskers and nanoparticles dimensions," *Carbohydrate Polymers* 84(1), 211-215. DOI: 10.1016/j.carbpol.2010.11.022

- Casu, B., Naggi, A., Torri, G., Allegra, G., Meille, S. V., Cosani, A., and Terbojevich, M. (1985). "Stereoregular acyclic polyalcohols and polyacetates from cellulose and amylose," *Macromolecules* 18(12), 2762-2767. DOI: 10.1021/ma00154a068
- Dong, X. M., Revol, J.-F., and Gray, D. G. (1998). "Effect of microcrystallite preparation conditions on the formation of colloid crystals of cellulose," *Cellulose* 5(1), 19-32. DOI: 10.1023/A:1009260511939
- Errokh, A., Magnin, A., Putaux, J.-L., and Boufi, S. (2018). "Morphology of the nanocellulose produced by periodate oxidation and reductive treatment of cellulose fibers," *Cellulose* 25(7), 3899-3911. DOI: 10.1007/s10570-018-1871-7
- Goetz, L., Mathew, A., Oksman, K., Gatenholm, P., and Ragauskas, A. J. (2009). "A novel nanocomposite film prepared from crosslinked cellulosic whiskers," *Carbohydrate Polymers* 75(1), 85-89. DOI: 10.1016/j.carbpol.2008.06.017
- Guigo, N., Mazeau, K., Putaux, J.-L., and Heux, L. (2014). "Surface modification of cellulose microfibrils by periodate oxidation and subsequent reductive amination with benzylamine: a topochemical study," *Cellulose* 21(6), 4119-4133. DOI: 10.1007/s10570-014-0459-0
- Kim, U.-J., Kuga, S., Wada, M., Okano, T., and Kondo, T. (2000). "Periodate oxidation of crystalline cellulose," *Biomacromolecules* 1(3), 488-492. DOI: 10.1021/bm0000337
- Kim, U.-J., Wada, M., and Kuga, S. (2004). "Solubilization of dialdehyde cellulose by hot water," *Carbohydrate Polymers* 56(1), 7-10. DOI: 10.1016/j.carbpol.2003.10.013
- Klemm, D., Heublein, B., Fink, H.-P., and Bohn, A. (2005). "Cellulose: Fascinating biopolymer and sustainable raw material," *Angewandte Chemie International Edition* 44(22), 3358-3393. DOI: 10.1002/anie.200460587
- Liimatainen, H., Visanko, M., Sirviö, J., Hormi, O., and Niinimäki, J. (2013). "Sulfonated cellulose nanofibrils obtained from wood pulp through regioselective oxidative bisulfite pre-treatment," *Cellulose*, 20(2), 741-749. DOI: 10.1007/s10570-013-9865-y
- Nechyporchuk, O., Belgacem, M. N., and Bras, J. (2016). "Production of cellulose nanofibrils: A review of recent advances," *Industrial Crops and Products* 93, 2-25. DOI: 10.1016/j.indcrop.2016.02.016
- Pan, S., and Ragauskas, A. J. (2014). "Enhancement of nanofibrillation of softwood cellulosic fibers by oxidation and sulfonation," *Carbohydrate Polymers* 111, 514-523. DOI: 10.1016/j.carbpol.2014.04.096
- Rajalaxmi, D., Jiang, N., Leslie, G., and Ragauskas, A. J. (2010). "Synthesis of novel water-soluble sulfonated cellulose," *Carbohydrate Research* 345(2), 284-290. DOI: 10.1016/j.carres.2009.09.037
- Rånby, B. G. (1949). "Aqueous colloidal solutions of cellulose micelles," *Acta Chemica Scandinavica* 3, 649-650. DOI: 10.3891/acta.chem.scand.03-0649
- Rocha, I., Ferraz, N., Mihranyan, A., Strømme, M., and Lindh, J. (2018). "Sulfonated nanocellulose beads as potential immunosorbents," *Cellulose*, 25(3), 1899-1910. DOI: 10.1007/s10570-018-1661-2
- Rodionova, G., Eriksen, Ø., and Gregersen, Ø. (2012). "TEMPO-oxidized cellulose nanofiber films: Effect of surface morphology on water resistance," *Cellulose* 19(4), 1115-1123. DOI: 10.1007/s10570-012-9721-5
- Sabzalian, Z., Alam, N., and van de Ven, T. G. M. (2014). "Hydrophobization and characterization of internally crosslink-reinforced cellulose fibers," *Cellulose* 21(3), 1381-1393. DOI: 10.1007/s10570-014-0178-6

- Segal, L., Creely, J. J., Martin, A. E., and Conrad, C. M. (1959). "An empirical method for estimating the degree of crystallinity of native cellulose using the X-Ray diffractometer," *Textile Research Journal* 29(10), 786-794. DOI: 10.1177/004051755902901003
- Shanmugarajah, B., Kiew, P. L., Chew, I. M. L., Choong, T. S. Y., and Tan, K. W. (2015). "Isolation of nanocrystalline cellulose (NCC) from palm oil empty fruit bunch (EFB): Preliminary result on FTIR and DLS analysis," *Chemical Engineering Transactions* 45, 1705-1710. DOI: 10.3303/CET1545285
- Sirviö, J. A., Visanko, M., Laitinen, O., Ämmälä, A., and Liimatainen, H. (2016). "Amino-modified cellulose nanocrystals with adjustable hydrophobicity from combined regioselective oxidation and reductive amination," *Carbohydrate Polymers* 136, 581-587. DOI: 10.1016/j.carbpol.2015.09.089
- Sirviö, J., Hyvakkö, U., Liimatainen, H., Niinimäki, J., and Hormi, O. (2011). "Periodate oxidation of cellulose at elevated temperatures using metal salts as cellulose activators," *Carbohydrate Polymers* 83(3), 1293-1297. DOI: 10.1016/j.carbpol.2010.09.036
- Sirviö, J., Liimatainen, H., Niinimäki, J., and Hormi, O. (2011). "Dialdehyde cellulose microfibrils generated from wood pulp by milling-induced periodate oxidation," *Carbohydrate Polymers* 86(1), 260-265. DOI: 10.1016/j.carbpol.2011.04.054
- Spedding, H. (1960). "Infrared spectra of periodate-oxidized cellulose," *Journal of the Chemical Society* 73, 3147-3152. DOI: 10.1039/jr9600003147
- Suganuma, S., Nakajima, K., Kitano, M., Yamaguchi, D., Kato, H., Hayashi, S., and Hara, M. (2008). "Hydrolysis of cellulose by amorphous carbon bearing SO₃H, COOH, and OH groups," *Journal of the American Chemical Society* 130(38), 12787-12793. DOI: 10.1021/ja803983h
- Sun, B., Hou, Q., Liu, Z., and Ni, Y. (2015). "Sodium periodate oxidation of cellulose nanocrystal and its application as a paper wet strength additive," *Cellulose* 22(2), 1135-1146. DOI: 10.1007/s10570-015-0575-5
- Sun, F., Liu, W., Dong, Z., and Deng, Y. (2017). "Underwater superoleophobicity cellulose nanofibril aerogel through regioselective sulfonation for oil/water separation," *Chemical Engineering Journal* 330, 774-782. DOI: 10.1016/j.cej.2017.07.142
- Thiangtham, S., Runt, J., and Manuspiya, H. (2019). "Sulfonation of dialdehyde cellulose extracted from sugarcane bagasse for synergistically enhanced water solubility," *Carbohydrate Polymers* 208, 314-322. DOI: 10.1016/j.carbpol.2018.12.080
- Visanko, M., Liimatainen, H., Sirviö, J. A., Heiskanen, J. P., Niinimäki, J., and Hormi, O. (2014). "Amphiphilic cellulose nanocrystals from acid-free oxidative treatment: Physicochemical characteristics and use as an oil-water stabilizer," *Biomacromolecules* 15(7), 2769-2775. DOI: 10.1021/bm500628g
- Voskoboinikov, I. V., Konstantinova, S. A., Korotkov, A. N., and Gal'braikh, L. S. (2011). "Process for preparing nanocrystalline cellulose," *Fibre Chemistry* 43(2), 125-128. DOI: 10.1007/s10692-011-9318-z
- Yang, H., Alam, N., and van de Ven, T. G. M. (2013). "Highly charged nanocrystalline cellulose and dicarboxylated cellulose from periodate and chlorite oxidized cellulose fibers," *Cellulose* 20(4), 1865-1875. DOI: 10.1007/s10570-013-9966-7
- Yang, H., Chen, D., and van de Ven, T. G. M. (2015). "Preparation and characterization of sterically stabilized nanocrystalline cellulose obtained by periodate oxidation of cellulose fibers," *Cellulose* 22(3), 1743-1752. DOI: 10.1007/s10570-015-0584-4

Zhao, H., and Heindel, N. D. (1991). "Determination of degree of substitution of formyl groups in polyaldehyde dextran by the hydroxylamine hydrochloride method," *Pharmaceutical Research* 8(3), 400-402. DOI: 10.1023/A:1015866104055

Article submitted: October 21, 2020; Peer review completed: December 27, 2020;
Revised version received and accepted: January 19, 2021; Published: January 21, 2021.
DOI: 10.15376/biores.16.1.1713-1725